IOP Publishing New J. Phys. 26 (2024) 093027 https://doi.org/10.1088/1367-2630/ad787d

New Journal of Physics
The open access journal at the forefront of physics

Deutsche Physikalische Gesellschaft DPG
IOP Institute of Physics

Published in partnership with: Deutsche Physikalische Gesellschaft and the Institute of Physics

OPEN ACCESS

RECEIVED
26 June 2024

REVISED
4 September 2024

ACCEPTED FOR PUBLICATION
9 September 2024

PUBLISHED
18 September 2024

PAPER

Engineering quasi-bound states in the continuum in asymmetric waveguide gratings

Torgom Yezekyan[1], **Sergejs Boroviks**[2], **Olivier J F Martin**[2] **and Sergey I Bozhevolnyi**[3,*]

[1] POLIMA—Center for Polariton-driven Light–Matter Interactions, University of Southern Denmark, Odense, Denmark
[2] Nanophotonics and Metrology Laboratory, Swiss Federal Institute of Technology Lausanne (EPFL), Lausanne, Switzerland
[3] Center for Nano Optics, University of Southern Denmark, Odense, Denmark
[*] Author to whom any correspondence should be addressed.

E-mail: seib@mci.sdu.dk

Keywords: grating waveguide couplers, bound states in the continuum, resonant electromagnetic interactions

Abstract

The occurrence of quasi-bound states in the continuum (qBIC) in all-dielectric asymmetric grating waveguide couplers with different degrees of asymmetry under normal light incidence is analysed from the viewpoint of identifying the most promising configuration for realizing the highest quality (Q) factor under the condition of utmost efficiency (i.e. total extinction). Considering asymmetric gratings produced by altering every *N*th ridge of a conventional (symmetric) grating coupler, we analyse different regimes corresponding to the interplay between diffractive coupling to waveguide modes and band gap effects caused by the Bragg reflection of waveguide modes. The symmetric and double- and triple-period asymmetric grating couplers are considered in detail for the same unperturbed two-mode waveguide and the grating coupler parameters that ensure the occurrence of total transmission extinction at the same wavelengths. It is found that the highest Q is expected for the double-period asymmetric grating, a feature that we explain by the circumstance that the first-order distributed Bragg resonator (DBR) is realized for this configuration while, for other configurations, the second-order DBR comes into play. Experiments conducted at telecom wavelengths for all three cases using thin-film Al_2O_3-on-MgF_2 waveguides and Ge diffraction gratings exhibit the transmission spectra in qualitative agreement with numerical simulations. Since the occurrence of considered qBIC can be analytically predicted, the results obtained may serve as reliable guidelines for intelligent engineering of asymmetric grating waveguide couplers enabling highly resonant, linear and nonlinear, electromagnetic interactions.

1. Introduction

Light diffraction on gratings that can excite propagating surface modes has been investigated since diffraction anomalies, i.e. anomalously rapid variations in the externally observable fields with respect to the angle of incidence or the incident light wavelength, were discovered by Wood in 1902 [1]. After realizing that two distinct types of anomalies exist, the Rayleigh type due to one of the spectral orders appearing at the grazing angle, and the resonance type due to possible guided complex waves supported by the grating configuration [2], the term of guided-mode resonances (GMRs) has been coined [3] followed by intensive and extensive investigations of different facets of GMRs (see, for example, recent reviews [4–6]). The developments related to the recently introduced [7] and widely explored [8–10] asymmetric metasurfaces supporting both bound and quasi-bound states in the continuum (BIC and qBIC) formed by the introduced grating asymmetry are particularly interesting and promising for realizing highly resonant, linear and nonlinear, electromagnetic interactions. Considering the investigated configurations, one notices that many of them rely explicitly [9] or implicitly [10] on the grating-enabled excitation of waveguide modes, thereby exploiting the GMR mechanism. Zooming in further on the configurations subjected to *normal* light incidence, which is arguably the most appealing in practice, one inevitably begins speculating on the interplay between diffractive coupling to waveguide modes and band gap effects caused by the Bragg reflection of waveguide modes [11].

Sharp features in transmission (reflection) GMR spectra being generated by the interference between zero-order transmission (reflection) and outcoupling of waveguide modes should be expected to be strongly affected by the band gap effects for normal light incidence. However, this aspect of realizing high quality (Q) resonances with metasurface-waveguide configurations has so far been largely unexplored, although it was first brought up when developing distributed feedback (semiconductor) lasers relying on distributed Bragg resonators (DBRs) employed for enforcing the mode selectivity [12, 13]. Furthermore, the realization of qBIC resonances (enabling ultrahigh-Q resonances [9]) by introducing the grating asymmetry implies the possibility of reaching infinitely high radiative Q for vanishingly small asymmetry [7], and thus infinitely high Q in all-dielectric systems [9]. At the same time, one might argue that the effect of infinitely narrow resonances produced by infinitely small perturbations cannot stay finite and consider the interplay between the efficiency and bandwidth of resonances, as well as their tradeoffs in different metasurface-waveguide configurations. This tradeoff, which is important, for example, for sensing applications [14], has not been considered for grating waveguide couplers (or, simply, waveguide gratings).

In this work, we consider the occurrence of qBIC and BIC resonances in all-dielectric grating waveguide couplers with different degrees of asymmetry under normal light incidence. In particular, we focus on identifying the most promising configuration for realizing the highest Q at the condition of the utmost efficiency (i.e. total transmission extinction and complete reflection). We introduce asymmetric gratings produced by altering every Nth ridge of a conventional (symmetric) grating coupler and analyse different regimes corresponding to the interplay between diffractive coupling to waveguide modes and band gap effects caused by the Bragg reflection of waveguide modes. We discuss the occurrence of BIC and qBIC from the perspective of the Friedrich–Wintgen mechanism of interfering resonances involving resonant modes coupled to the same radiation channel [15]. We investigate in detail a practical configuration of thin-film Al_2O_3-on-MgF_2 waveguides and 1200 nm-period Ge diffraction gratings operating at telecom wavelengths. Detailed numerical simulations for close to normal plane TE-wave incidence and preliminary experiments are reported (a comprehensive theoretical framework for such platforms can be found in [9]). We find that the highest Q under the condition of total extinction is expected for the double-period asymmetric grating, a feature that we explain by the fact that the first-order DBR is realized for this configuration while, for other configurations, the second-order DBR comes into play. With the considered BIC and qBIC predicted analytically with high accuracy, the results obtained will serve as reliable guidelines for engineering asymmetric grating waveguide couplers enabling highly resonant electromagnetic interactions.

2. Qualitative considerations

We begin by considering a planar (two-dimensional) thin-film waveguide with an asymmetric grating on its top, which is constructed in such a way that the grating asymmetry can gradually be adjusted by varying the width of only one ridge in the grating supercell, figure 1(a).

The waveguide is assumed to support the propagation of at least one mode at the wavelength range of interest (telecom, in our case) that can be excited by an electromagnetic wave incident on the diffraction grating. While the use of grating couplers for efficient excitation of optical guided waves in thin-film waveguides has been known for more than 50 years [2, 16], their exploitation for realizing highly efficient resonant transmission and/or reflection of freely propagating waves is much more recent, with many technological applications being currently under intensive development (see a comprehensive review [4]). From the latter perspective, the waveguide diffraction gratings are conventionally termed as resonant waveguide gratings (RWGs). In this work, we study a particular case, viz., RWG excitation of the standing waveguide mode formed by interference of two counterpropagating waveguide modes that are resonantly excited under *normal* light incidence *and* Bragg reflected one into another, figure 1(b), resulting in the occurrence of BIC and qBIC resonances. In this configuration, the RWG can be considered as a DBR, functioning like the well-known DBRs exploited in the 70 s for mode selection in distributed feedback semiconductor lasers [12, 13]. It should be noted that the efficient narrowband transmission and/or reflection can also be realized at off-normal light incidence [2, 16], resulting in the phase-matched excitation of a propagating (away from the excitation domain) waveguide mode, figure 1(c). This Fano interference phenomenon should not be confused with any of the resonances, because the occurrence of resonance implies the existence of resonant field configuration, storing the energy and sustaining without the external excitation during the time determined by the resonance fidelity (quality) Q.

Efficient excitation of counterpropagating waveguide modes under normal incidence (from the air side) requires that the waveguide mode wavelength, λ_w, is equal to the grating period: $\lambda_w = \Lambda = N\Lambda_0$ (figure 1). Here, we consider the mode excitation only in the first diffraction order, which is a much more efficient process than the second-order mode excitation. Furthermore, the second-order waveguide mode excitation might result in the first-order excitation of free propagating (away from the waveguide) waves. If we

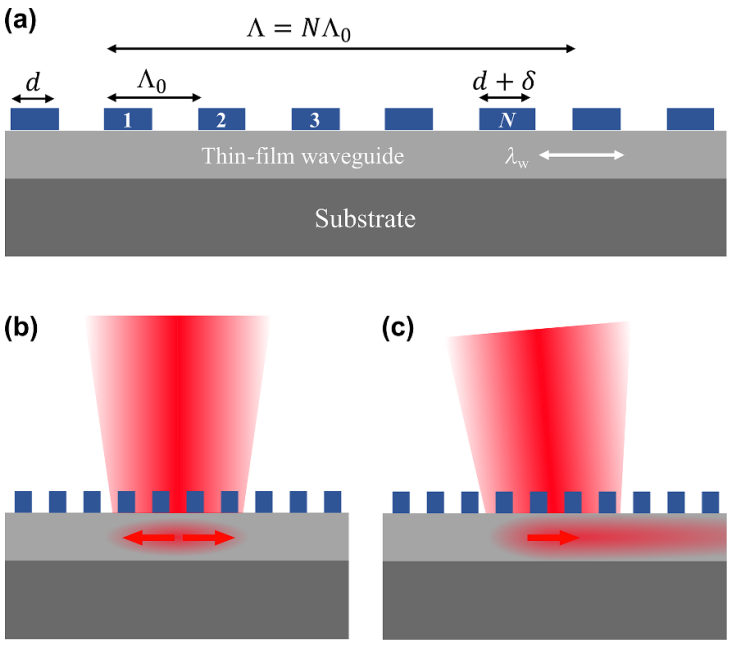

Figure 1. Schematic of the considered thin-film waveguide configuration with the asymmetric grating on its top (a), featuring the supercell period of $\Lambda = N\Lambda_0$. The asymmetry is introduced by increasing one supercell element in width from d to $d + \delta$. The waveguide mode wavelength is denoted by λ_w. Resonant excitation of the standing waveguide mode formed by two counterpropagating waveguide modes in a DBR under normal light incidence (b), as opposed to the phase-matched excitation of a propagating waveguide mode under oblique light incidence (c).

additionally require the DBR realization, i.e. Bragg reflection of counterpropagating waveguide modes, in the mth Bragg reflection order formed by the *unperturbed* symmetric grating with the period Λ_0, we obtain the following condition: $2\Lambda_0 = m\lambda_w$. These two conditions will be met when $Nm = 2$, a requirement that ensures both the first-order excitation of two counterpropagating waveguide modes and their Bragg reflection one into another, i.e. the DBR excitation.

The above requirement can only be met in two cases, when considering integer positive numbers: (*i*) $N = 1$ and $m = 2$; and (*ii*) $N = 2$ and $m = 1$. In both cases, the DBR realization is associated with the avoided crossing of Bloch mode dispersion curves, i.e. with the band gap effect [17]. The corresponding standing-wave solutions are expected to feature the intensity maxima at the places of high or low refractive index, corresponding to the low or upper dispersion branches, in accordance with the variational principle [17]. Consequently, it should be expected that the radiation leakage, the process that is inverse to the waveguide mode excitation, stems from two waves generated by the counterpropagating waveguide modes, which can interfere constructively or destructively. The latter case of vanishing radiation leakage is responsible for the BIC formation due to the FW mechanism of interfering resonances [15]. We consider these two cases in more detail in the following.

The first case, $N = 1$, corresponds to the *symmetric* ($\delta = 0$) unperturbed grating with a relatively large period $\lambda_w = \Lambda_0$, figure 1(a). These gratings were previously extensively used in distributed feedback lasers for enforcing mode selection [12, 13]. It has been shown that, for the second order DBR, two radiative contributions due to the first-order diffraction of counterpropagating waveguide modes, being of a similar magnitude, add up or cancel each other depending on the energy side of the band gap. Specifically, the contributions cancel each other on the low energy side of the band gap, resulting in the lasing mode, while the competing mode on the high energy side is suppressed (outcompeted) due to relatively large radiation losses [12, 13]. It is thus expected that the BIC is formed at the low energy side of the band gap, whereas the resonance occurring at the high energy side is subjected to radiative loss, thus representing the qBIC.

The second case, $N = 2$ and $m = 1$, corresponds to the *asymmetric* ($\delta \neq 0$) grating with a relatively small basic period $\lambda_w = 2\Lambda_0$ in which the array period is doubled by the introduced asymmetry, figure 1(a), resulting in the first order DBR. The corresponding band gap associated with the anti-crossing of the Bloch mode dispersion curves opens again the possibility for realizing constructive or destructive interferences between two outcoupled waves generated by the counterpropagating waveguide modes, depending on the band gap side. The interference outcome is determined by the relative signs of the corresponding Fourier components in the grating profile representation [12, 13] or, in the FW mechanism of interfering resonances, by the relative signs of the coupling matrix elements [15]. In both cases, the reversal in the positions of BIC

and qBIC (with respect to the previous case) can be expected, since these signs should depend on the grating symmetry.

Next, we consider the realization of the Bragg resonance of the mth order by the grating supercell, i.e. by the *asymmetric* (perturbed) grating with the period $\Lambda = N\Lambda_0$, thus obtaining the following requirement $2\Lambda = m\lambda_w$. Along with the condition of the mode excitation in the first diffraction order, $\lambda_w = \Lambda$, we obtain a very simple requirement: $m = 2$. This implies that, for *any* number N of ridges constituting the grating supercell, figure 1(a), the DBR is realized in the second order of the Bragg resonance. This situation for $N = 1$ is, in fact, already considered above as the first case. It is however interesting that, in the second case, the considered band gap is a *combined* result of the first order Bragg resonance formed by the strongest grating component associated with the unperturbed symmetric grating with the period Λ_0 *and* the second order Bragg resonance formed by the grating supercell with the period $\Lambda = 2\Lambda_0$. The next in line case with $N = 3$ would therefore represent a new configuration, with an asymmetric grating providing the first-order coupling (and radiation loss) and the second order DBR. Since the outcoupling of the excited waveguide modes in this case is also provided by an asymmetric grating, one would expect finding similar (to the second case) locations for the BIC and qBIC.

Concluding this section with the qualitative considerations, we note that the cases with $N > 3$ are only slightly different from the third case with $N = 3$. In all these cases, the period of the unperturbed symmetric grating Λ_0 is significantly smaller than the waveguide mode wavelength, because $\lambda_w = \Lambda = N\Lambda_0$, so that the presence of unperturbed grating can simply be factored in the waveguide configuration by adding a corresponding overlayer in accordance with the effective medium approach [16]. Therefore, in our model configurations with asymmetric gratings produced by altering every Nth ridge of a conventional (symmetric) grating coupler, we have identified only 3 cases: $N = 1$, 2 and 3, that are substantially different from the viewpoint of interplay between the diffractive coupling to counterpropagating waveguide modes and their Bragg reflection mediated coupling within the same grating.

3. Results

Here we present the results of detailed numerical simulations pertaining to the three different cases discussed in the previous section. Both the eigenmodes and transmission spectra are calculated by commercial software Comsol Multiphysics based on finite-element-method with a typical mesh of 80 nm. Floquet periodic conditions were used on the boundaries of the unit cell. The three considered configurations (figure 2) are chosen in accordance with the following conditions: (a) the 500 μm-thick MgF_2 substrate and 1.2 μm-thin waveguiding layer of Al_2O_3 ensure the existence of at least one TE-mode (the electric field is parallel to the material interfaces) at telecom wavelengths and correspond to the actual substrates fabricated by thin-film deposition for the proof-of-principle experiments; (b) all configurations have the same supercell grating period of 1200 nm to ensure the mode excitation at normal incidence of light at the same (or very close) telecom wavelengths; (c) all gratings consist of 50 nm-high Ge ridges, facilitating their simultaneous fabrication; and (d) the ridge widths are chosen to ensure that the DBRs (in all three cases) are formed at the same wavelengths *and* would result in the complete extinction of the light transmission, at least in the simulations (figure 2).

The transmission spectra at normal incidence in all cases exhibit Fano-like features associated with the DBR excitation with the minimum being to the qBIC excitation. It is however not possible from these spectra *alone* to determine which, low or high, energy side of the band gap these minima correspond to. Importantly, the DBR bandwidths appear markedly different: the bandwidths corresponding to the asymmetric gratings formed by dimerization and trimerization are significantly narrower than that observed with the symmetric grating (for the fundamental mode approximately 26 nm, 3.7 nm and 8.7 nm with the symmetric, dimerized and trimerized gratings respectively). It can be explained by the circumstance that, in the symmetric grating, a relatively weak band gap effect is realized in the second order of the Bragg resonance, while relatively strong radiation loss occurrs in the first order diffraction. At the same time, the band gap effect in the double-period grating is associated with the combined effect of the first order Bragg resonance formed by the strong symmetric grating component and the second order Bragg resonance formed by the grating supercell. The combined effect is probably the main reason for the DBR bandwidth for the double grating being notably narrower than that for the triple grating.

This clear distinction between the considered three cases is related to the imposed condition of complete extinction (zero transmission) that requires sufficiently strong in- and outcoupling, since the outcoupled wave should match in magnitude the directly transmitted wave in order for these two waves to cancel each other in destructive interference. In this case, stronger band gaps would result in more roundtrips in the DBR and thereby longer effective propagation length, ultimately leading to narrower resonances and larger Q. The first ($N = 1$) and third ($N = 3$) cases are similar from the viewpoint of the DBR being realized in the

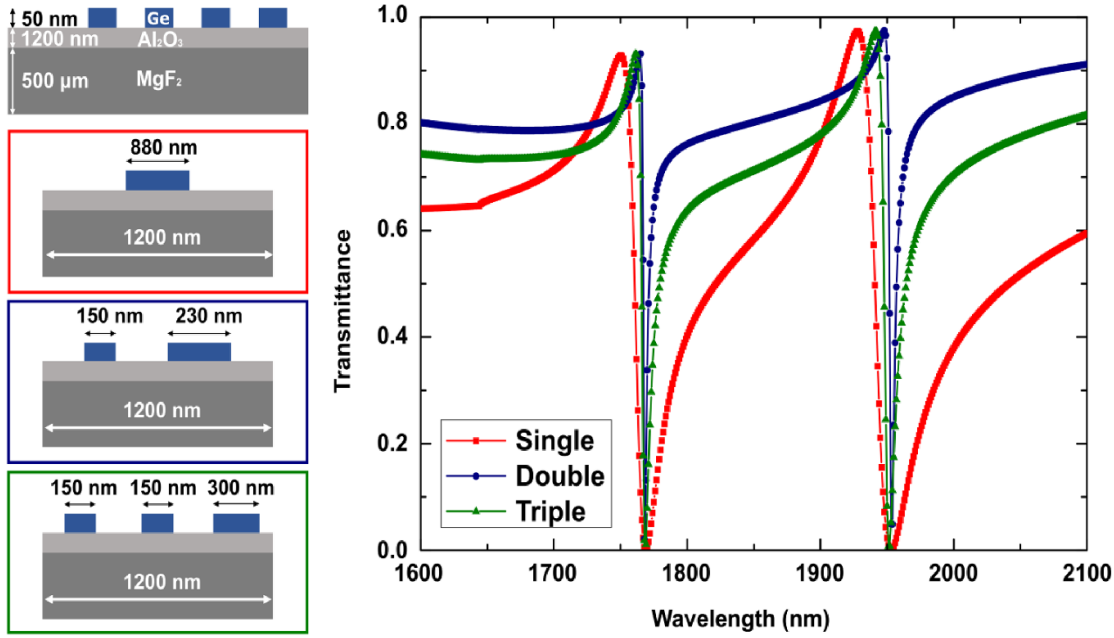

Figure 2. Transmission spectra at normal light incidence (right panel) shown with squares, circles and triangles correspondingly for the three chosen configurations (left panel), representing the symmetric (single ridge within the grating period), dimerized (double) and trimerized (triple) gratings. Each case exhibits two transmission extinction corresponding to the excitation of the fundamental (right minimum) and first-order (left minimum) TE modes in the considered waveguide. In simulations the refractive index (with disperssion) of Ge (values around 4) was taken from [18]. Refractive indexes of 1.65 for Al_2O_3 and 1.37 for MgF_2 were taken from [19, 20] respectively. Due to small disperssion, it was diregarded for these materials (at wavelength extremes that we used (namely 1600 nm and 2100 nm) the refractive indices are as follows: 1.658 and 1.65 for Al_2O_3; 1.37 and 1.367 for MgF_2).

second-order band gap, but the second-order Bragg reflection by a symmetric grating is understandably weaker than the second-order Bragg reflection by an asymmetric grating, under the condition of their first-order outcoupling being of similar strength.

To gain further understanding of the underlying physical mechanisms involved in the DBR formation and nature of the observed resonances, we consider the Bloch mode dispersion curves and transmission spectra in the vicinity of normal incidence (figure 3). The formation of the band gap is confirmed with the dispersion calculations, with the BIC positions with respect to the band gap being identified by calculating the quality factors that appear diverging in the BIC cases, figures 3(a)–(c). The band gap sides opposite to the BIC correspond to the qBIC, whose excitation causes the transmission minima (figure 2). The relative positions of BIC and qBIC correspond to those described in the above section with qualitative considerations, confirming the switching of their locations when changing from symmetric, figure 3(a), to asymmetric, figures 3(b) and (c), gratings. It is also seen that the standing wave intensity patterns exhibit the expected symmetry, featuring the intensity maxima at the places of high or low refractive indexes (associated with the locations of high index Ge ridges) for correspondingly low or upper dispersion branches, as predicted by the variational principle [17], an effect that is better observed in figures 4(a)–(c).

The largest band gap is observed for the symmetric grating, figure 3(a), that features the lowest Q (figure 2), seemingly contradicting the above conclusion on stronger band gaps resulting in larger Q. In fact, one should be very careful when comparing symmetric and asymmetric gratings and should consider the inherent difference in the physics of band gap formation seen in the different positions of BIC and qBIC as noted above, figures 3(a)–(c). Comparing asymmetric gratings, figures 3(b) and (c), the band gap in the second case is significantly larger than that in the third case, in agreement with the transmission minimum being notably narrower in the second case (figure 2). We explain this difference between double and triple gratings by the fact that, as remarked above, the band gap in the double grating is a combined result of the first order band gap formed by the strongest grating component of the unperturbed symmetric grating and the second order band gap formed by the grating supercell. The band gap in the triple grating is caused only by the second order Bragg resonance formed by the grating supercell, and thus the band gap is expected to be narrower than that in the second case.

The assignment of the band gap sides to either the BIC or qBIC can further be verified by analysing the dispersion curves in the immediate vicinity of normal incidence. Indeed, for a small non-zero angle of incidence, the occurrence of two transmission minima (instead of one observed at normal incidence) is

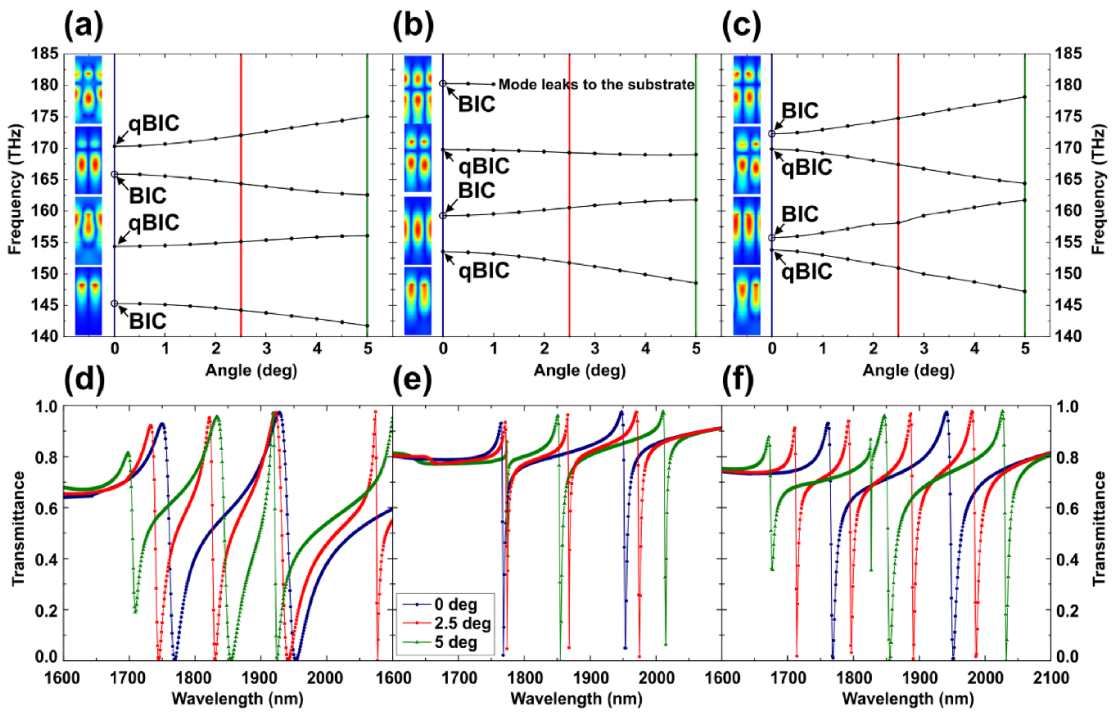

Figure 3. Dispersion curves (a)–(c) and transmission spectra (d)–(f) calculated in the vicinity of normal incidence: (a) and (d) correspond to single, (b) and (e) to double and (c) and (f) to triple gratings (see figure 1). Different angles of incidence: 0°, 2.5° and 5– are shown with circles, squares and triangles, respectively. Insets show, within the 1200 nm-wide unit cell, the standing wave intensity patterns calculated for both TE modes at the BIC and qBIC positions, i.e. for normal incidence, overlaid with the grating-atop-waveguide configurations.

markedly asymmetric with respect to that found at normal incidence, since following the qBIC branch results in a much smaller shift in the wavelength associated with the transmission minimum compared to that observed when following the BIC branch. This difference is caused by the band gap and is expectedly larger for larger band gaps.

Thus, in the first case, the transmission minimum is observed for the fundamental mode at normal incidence at ∼1950 nm (figure 2). This minimum gives rise to two for the 2.5°-angle-incidence: one at ∼1940 nm and another at ∼2080 nm, figure 3(d), exhibiting, respectively, ∼10 and 130 nm wavelength shifts toward shorter and longer wavelengths. An order of magnitude smaller wavelength shift toward lower frequencies indicates unambiguously the qBIC occurrence at the high energy side of a relatively large band gap, figure 3(a). The opposite trends in wavelength splits are observed in the second and third cases. Thus, in the second case, the fundamental mode transmission minimum (at ∼1950 nm) gives rise to two for the 2.5°-angle-incidence: one at ∼1865 nm and another at ∼1975 nm, figure 3(e), exhibiting, correspondingly, ∼ 85 and 25 nm wavelength shifts toward shorter and longer wavelengths. A much larger wavelength shift toward higher frequencies indicates unambiguously the qBIC occurrence at the low energy band gap side, figure 3(b). The same trend in the wavelength splits is also observed in the third case, figure 3(f), albeit the asymmetry in the splits is less pronounced because of relatively small band gaps, figure 3(c). Therefore, the minimum positions observed in the wavelength spectrum for very small angles of incidence explicitly reveal the band gap and allow one to properly assign qBIC or BIC to different dispersion branches, figures 3(a)–(c).

Concluding the discussion of the transmission spectra at close to normal incidence, we would like to draw the attention toward the widths of the transmission minima. For all three gratings, the two transmission minima occurring for nonzero angles of incidence are noticeably narrower than the corresponding qBIC-related transmission minimum observed at normal incidence, figures 3(d)–(f). This narrowing of the transmission minima is consistent with the FW mechanism of interfering resonances [15] and its particular case describing the suppression of one of two modes in second-order distributed feedback lasers by first-order radiation losses [12, 13]. Indeed, according to the FW mechanism, the BIC/qBIC occurrence (at low or high energy sides) is determined by the relative signs of the coupling matrix elements [15] associated with similar strength contributions from the first-order diffraction of counterpropagating waveguide modes [12, 13]. At the qBIC (BIC), these contributions interfere constructively (destructively) resulting in relatively large (negligibly small) radiation losses and thus wide (infinitely narrow and shallow) transmission minima.

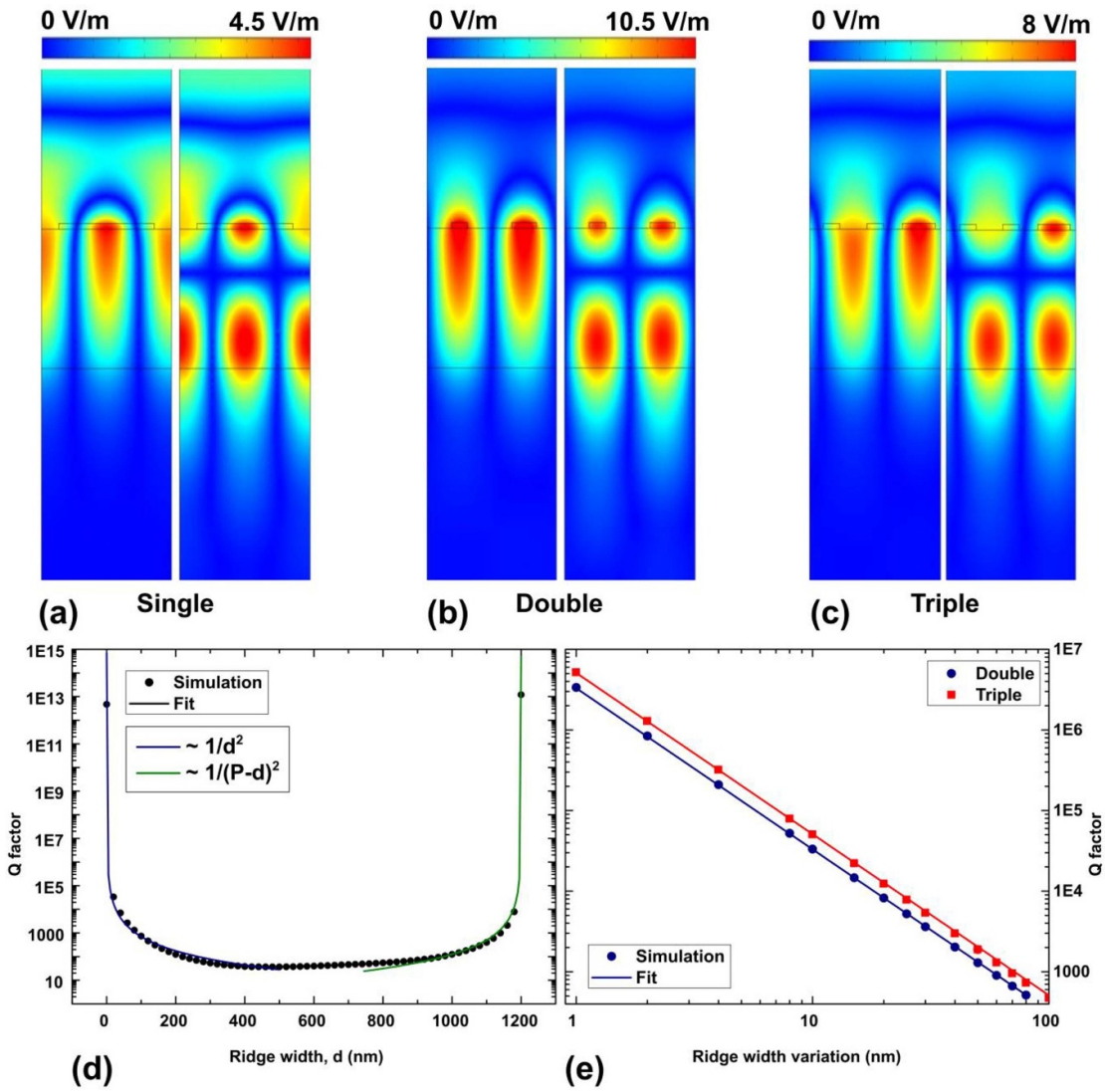

Figure 4. The TE field magnitude distributions at qBIC resonances for the symmetric (a) and asymmetric (b), (c) gratings calculated for the nominal grating parameters (figure 2) and incident electric field of 1 V/m, along with the corresponding quality factors calculated as functions of the critical geometrical parameters of the considered configurations for single (d) and double and triple (e) gratings. For all cases (d), (e), Q-factors are shown only for the fundamental (low frequency) waveguide modes to avoid overlap with very similar dependencies for the first order (high frequency) waveguide modes.

For any nonzero incident angle, the mode radiative leakage (diffractive outcoupling) occurs *only* for one waveguide mode—the waveguide mode that is excited at a particular frequency away from normal incidence, figure 1(c). The immediate consequence expected for normal light incidence is *halving* the widths of transmission minima, a phenomenon that explains the above observations, figures 3(d)–(f).

The qBIC resonances realized in the considered three cases are expected to exhibit different resonance features because of rather different origins as previously discussed with qualitative considerations. We analysed using numerical simulations the field magnitude distributions and electromagnetic energy storage by these resonances, as well as their quality factors as functions of the key geometrical parameters (figure 4).

Considering the field magnitude maxima locations with respect to the Ge (high index) ridge positions and bearing in mind the variational principle [17], one can realize that the qBIC in the first case should occur at the high energy band gap side, figure 4(a), whereas the qBICs in the second and third cases should occur at the low energy band gap sides, figures 4(b) and (c), as indeed was established above, figures 3(a)–(c). The calculated TE mode field magnitude spatial distributions reveal resonantly enhanced modes, with much stronger fields being formed in the asymmetric gratings, figures 4(b) and (c), than those found in the degenerate case of a symmetric grating, figure 4(a). Interestingly, the band gap in both degenerate and triple-period cases is of the second order, but the resonant field magnitudes are much stronger for the latter.

This difference is consistent with the transmission minimum being notably narrower (and thus Q notably larger) for the asymmetric case (figure 2). The field enhancement effects vary typically in agreement with the resonance quality Q that reflects the number of resonant field oscillations in a resonator.

The quality resonance factors are calculated for qBICs in all three cases (for normal incidence of light) as functions of the critical geometrical parameters, i.e. the parameters whose vanishing would cause the band gap and qBIC disappearance. It should be emphasized that, when following the evolution of Q, both the resonance wavelength and efficiency are changing in comparison with those shown in figure 2. The changes in resonance wavelength are insignificant, being related to changes in the mode effective index due to changes in the waveguide loading by the grating. But the changes in the resonance efficiency, i.e. in the depth of the transmission minimum, are profound, with the transmission dip asymptotically disappearing along with vanishing critical parameters. This is the reason for conducting the comparison of three cases under the condition of complete extinction in this work. One might consider comparing the three cases from the viewpoint of reaching the highest efficiency under the condition of featuring the same resonance quality Q. This would represent an interesting route to follow by choosing a set of different Qs to be realized in the three configurations (by finding suitable grating parameters) and comparing the resulting resonance efficiencies (transmission depths) achieved in these conditions.

In the first case of the symmetric (single) grating, the grating itself will disappear if the ridge width d vanishes, or if d increases so that the gap between ridges, Λ_0–d, would go to zero. It is seen that, in both limits of very narrow and very wide ridges, the Q-factor dependencies feature the inverse quadratic dependencies, figure 4(d). In the absence of absorption, the leakage radiation is the only dissipation channel, whose strength is proportional to the scattering strength, i.e. to the squared polarizability and thus squared ridge volume and thus squared ridge width, thereby qualitatively explaining the trends observed, figure 4(d). Interestingly, the radiative Q-factor of qBICs in asymmetric metasurfaces depends on the asymmetry parameter in the same fashion [12, 13]. For the asymmetric (double and triple) gratings in our case, the Q-factor dependencies calculated as a function of the ridge width variation δ (figure 1), which is proportional to the asymmetry parameter δ/d, feature the inverse quadratic dependencies, $Q \sim 1/\delta^2$ as expected, figure (e). One can argue that also in these cases the leakage radiation strength should be proportional to the strength of scattering by an additional piece of ridge (of size δ) that transforms a symmetric grating of period Λ_0, which does not couple the waveguide modes out, into the double or triple gratings. The inverse quadratic dependence observed follows then straightforwardly as in the first case of the symmetric grating, resulting in the inverse quadratic dependence with respect to the effective perturbation volume [9].

Finally, we present in the following the results of the proof-of-principle experiments. To fabricate the samples of the designed grating configuration (figure 2), we first coated 1200 nm of Al_2O_3 (RF-sputtering of using SPIDER 600 from Pfeiffer, thickness verified subsequently, using optical profilometer FilMetrics F54-XY-200) on a 500 μm-thick MgF_2 substrate. Next, the grating patterns were exposed in PMMA resist using electron beam lithography. Evaporation of 50 nm-thick Ge layer (Cryofox 600 Explorer from Polyteknik), followed by lift-off in acetone, yields gratings of a very good quality, figures 5(a)–(c). The schematics of the setup used for transmission measurements is shown in figure 5(d). The transmission spectra were measured by Ocean Insight NIRQuest +1.7 spectrometer with InGaAs linear array. As a light source we used SuperK EXTREME supercontinuum laser from NKT Photonics (ranging from 400 to 2400 nm), where the visible part of the spectrum was filtered out by long-pass filter. In all measurements the illumination of the sample (DUT in figure 5(d)) was realized with collimated beam incidence covering the whole area with gratings, thereby imitating a plane wave incidence. For the collection, a x20 objective was used (numerical aperture of 0.6) with a corresponding pinhole, to spatially select only the central part of the gratings. For the references we measured the transmission through the substrate (bulk MgF_2 with 1.2 μm-thin Al_2O_3 film) and normalized to that value. Although conducting the optical characterization was rather challenging, because it requires large 'perfect' gratings and collimated wide incident beams, i.e. as close to plane waves as possible, the main features are well reproduced: (i) two waveguide modes are found in the considered wavelength range; (ii) the narrowest (widest) transmission minima are observed for the double asymmetric (symmetric) grating, figure 5(e); and (iii) the transmission minima give rise to two minima each for a non-zero angle of light incidence, figure 5(f). The observed differences between the experimental data and simulated results for the transmission minima locations and depths can be explained by deviations of layer thicknesses from the nominal values and fabrication inaccuracies. Additionally, it was difficult to experimentally control the angle of incidence for telecom light with the high precision required for these

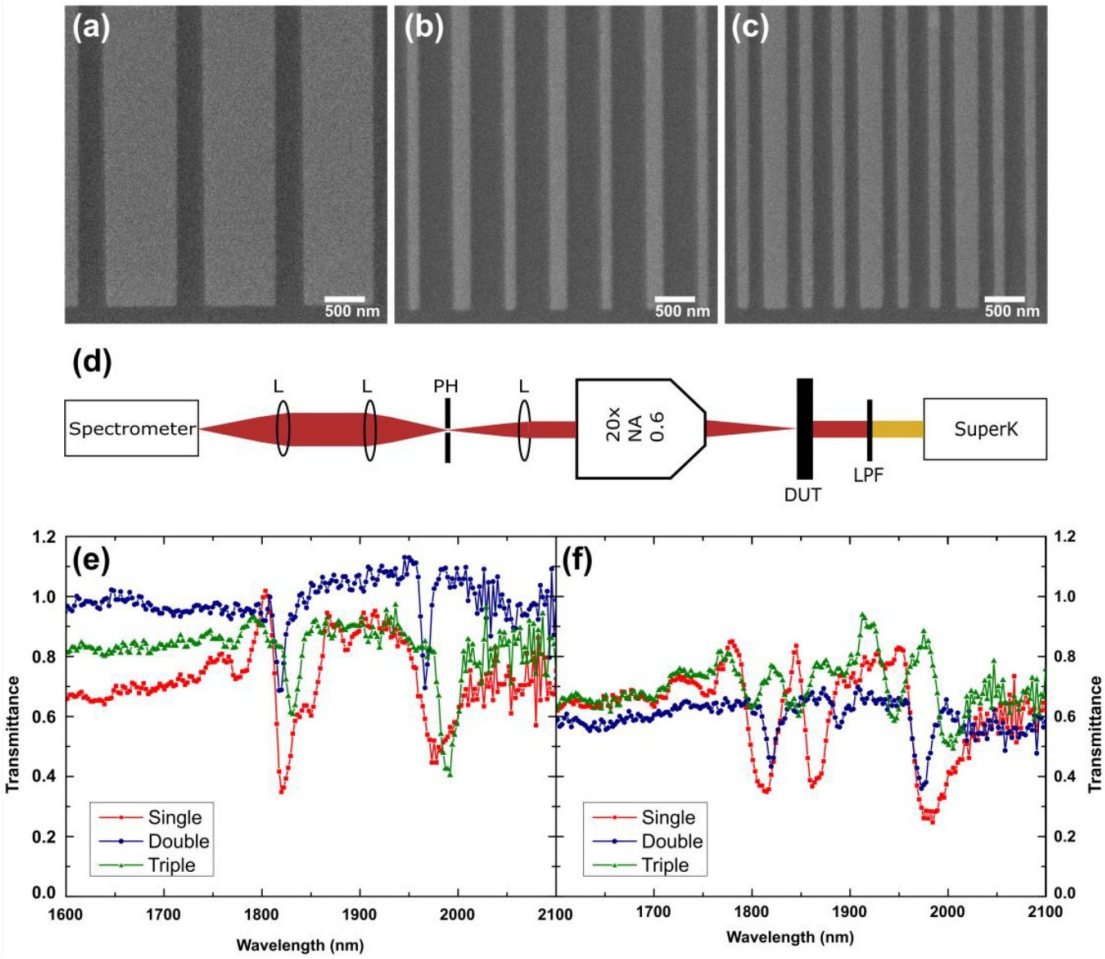

Figure 5. The scanning electron microscopy (SEM) images of the symmetric (a), dimerized (b) and trimerized (c) gratings fabricated with the (close to) nominal grating parameters (figure 2); the schematics of the experimental setup used for transmission measurements (d), as well as the transmission spectra of the three structures (a)–(c) at telecom wavelength range measured for the normal (e) and close to by ∼2° (f) light incidences. Different cases (single, double and triple) are shown with squares, circles and triangles, respectively.

narrow resonances. It is conceivable that the broadening of the transmission minimum observed for normal incidence in the first case (single grating) is caused by deviation from the normal incidence, figure 5(e).

4. Conclusions

We have studied, with simulations and experiments, the transmission optical spectra of symmetric and asymmetric diffraction grating waveguide couplers in the telecom wavelength range. We have analysed different regimes corresponding to the interplay between diffractive coupling to waveguide modes and band gap effects caused by the Bragg reflection of waveguide modes. We have established the underlying physical mechanisms involved in the formation of BIC and qBIC resonances on the opposite band gap sides, from the perspective of the FW mechanism of interfering resonances [15]. The symmetric and double- and triple-period asymmetric grating couplers were considered in detail for the same unperturbed two-mode waveguide and the grating coupler parameters that ensure the occurrence of complete transmission attenuation extinction at the same wavelengths. It was found that the highest Q is expected for the double-period asymmetric grating, a feature that we explained by the circumstance that the first-order DBR is realized for this configuration while, for other configurations, the second-order DBR comes into play. When considering nonzero angles of incidence, we have discovered that both transmission minima resulting from the qBIC split are ∼2 times narrower than the unsplit transmission minimum observed at normal

incidence, a very important feature that we explained using the FW mechanism of interfering resonances [15]. Interestingly, at the same time, the band gaps formed continue, in all cases, to be related to the forbidden frequencies, i.e. frequencies within band gaps remain inaccessible even for nonzero angles of light incidence. We have also conducted proof-of-principle experiments in the telecom wavelength range using thin-film Al_2O_3-on-MgF_2 waveguides and Ge diffraction gratings, showing that, for all three cases, the main features found in the measured transmission spectra are in overall agreement with numerical simulations.

From the viewpoint of potential applications, narrowing the transmission minima in both symmetric and asymmetric RWGs for nonzero angles of incidence can have far reaching implications to using RWGs for sensing and enhancing nonlinear interactions [4]. It would be very interesting to explore nonlinear interactions, such as second-harmonic generation [8] and non-reciprocal non-linear transmission [10], using the waveguide based qBIC discussed in this work. Interestingly, the FW mechanism of interfering resonances was also very recently brought up in the study on superscattering that emerges from the BIC physics [21]. Overall, we believe that, with the considered BIC and qBIC being predicted analytically with high accuracy, the results obtained would serve as reliable guidelines for intelligent engineering of asymmetric grating waveguide couplers enabling highly resonant, linear and nonlinear, electromagnetic interactions.

Data availability statement

All data that support the findings of this study are included within the article (and any supplementary files).

Acknowledgment

The authors would like to acknowledge Professor Yuri Kivshar (Australian National University) for insightful discussions.

Research funding

One of co-authors (TY) acknowledges the support from the Center for Polariton-driven Light-Matter Interactions (POLIMA) funded by the Danish National Research Foundation (Project No. DNRF165).

ORCID iDs

Torgom Yezekyan https://orcid.org/0000-0003-2019-2225
Sergejs Boroviks https://orcid.org/0000-0002-3068-0284
Olivier J F Martin https://orcid.org/0000-0002-9574-3119
Sergey I Bozhevolnyi https://orcid.org/0000-0002-0393-4859

References

[1] Wood R W 1902 Remarkable spectrum from a diffraction grating *Phil. Mag.* **4** 396–402
[2] Hessel A and Oliner A A 1965 A new theory of Wood's anomalies on optical gratings *Appl. Opt.* **10** 1275–97
[3] Wang S S, Magnusson R, Bagby J S and Moharam M G 1990 Guided-mode resonances in planar dielectric-layer diffraction gratings *J. Opt. Soc. Am.* A **7** 1470–5
[4] Quaranta G, Basset G, Martin O J F and Gallinet B 2018 Recent advances in resonant waveguide gratings *Laser Photonics Rev.* **12** 1800017
[5] Koshelev K, Bogdanov A and Kivshar Y 2019 Meta-optics and bound states in the continuum *Sci. Bull.* **64** 836–42
[6] Huang L, Xu L, Powell D A, Padilla W J and Miroshnichenko A E 2023 Resonant leaky modes in all-dielectric metasystems: fundamentals and applications *Phys. Rep.* **1008** 1–66
[7] Koshelev C K, Lepeshov S, Liu M, Bogdanov A and Kivshar Y 2018 Asymmetric metasurfaces with high-Q resonances governed by bound states in the continuum *Phys. Rev. Lett.* **121** 193903
[8] Kang M, Liu T, Chan C T and Xiao M 2023 Applications of bound states in the continuum in photonics *Nat. Rev. Phys.* **5** 659–78
[9] Huang L *et al* 2023 Ultrahigh-Q guided mode resonances in an all-dielectric metasurface *Nat. Commun.* **14** 3433
[10] Cotrufo M, Cordaro A, Sounas D L, Polman A and Alù A 2024 Passive bias-free non-reciprocal metasurfaces based on thermally nonlinear quasi-bound states in the continuum *Nat. Photon.* **18** 81–90
[11] Gallinet B, Siegfried T, Sigg H, Nordlander P and Martin O J 2013 Plasmonic radiance: probing structure at the ångström scale with visible light *Nano Lett.* **13** 497–503
[12] Kazarionov R F and Suris R A 1973 Injection heterojunction laser with a diffraction grating on its contact surface *Sov. Phys.* **6** 1184–9
[13] Kazarinov R F and Henry C H 1985 Second-order distributed feedback lasers with mode selection provided by first-order radiation losses *IEEE J. Quantum Electron.* **21** 144–50
[14] Zhang S, Wong C L, Zeng S, Bi R, Tai K, Dholakia K and Olivo M 2021 Metasurfaces for biomedical applications: imaging and sensing from a nanophotonics perspective *Nanophotonics* **10** 259–93
[15] Friedrich H and Wintgen D 1985 Interfering resonances and bound states in the continuum *Phys. Rev.* A **32** 3231–42
[16] Dakss M L, Kuhn L, Heidrich P F and Scott B A 1970 A grating coupler for efficient excitation of optical guided waves in thin films *Appl. Phys. Lett.* **16** 523–5

[17] Joannopoulos J D, Meade R D and Winn J N 1995 *Photonic Crystals* (Princeton University Press)
[18] Yezekyan T E, Zenin V A, Thomaschewski M, Malureanu R and Bozhevolnyi S I 2023 Germanium metasurface assisted broadband detectors *Nanophotonics* **12** 2171–7
[19] Boidin R, Halenkovič T, Nazabal V, Beneš L and Němec P 2016 Pulsed laser deposited alumina thin films *Ceram. Int.* **42** 1177–82
[20] Zheng Q, Wang X and Thompson D 2023 Temperature-dependent optical properties of monocrystalline CaF_2, BaF_2 and MgF_2 *Opt. Mater. Express* **13** 2380–91
[21] Valero A C, Shamkhi H K, Kupriianov A S, Weiss T, Pavlov A A, Redka D, Bobrovs V, Kivshar Y and Shalin A S 2023 Superscattering emerging from the physics of bound states in the continuum *Nat. Commun.* **14** 4689